

**Military Technical College
Kobry El-Kobbah,
Cairo, Egypt.**



**16th International Conference
on Applied Mechanics and
Mechanical Engineering.**

HEAT TRANSFER CHARACTERISTICS OF WATER FLOWING THROUGH SINGLE AND DOUBLE STACK RECTANGULAR MICROCHANNELS

I. Elbadawy**, S. Anbr* and M. Fatouh***

ABSTRACT

The generated heat in electronic components whenever electric current flows through them causes their temperatures to rise. In order to minimize the temperature rise of the components, the dissipation of heat is necessary for their proper functioning. Copper based microchannel heat sinks have various advantages such as combine high material compatibility, high surface area per unit volume ratio and large potential heat transfer performance with highly sophisticated and economic fabrication process. Thus, the present work aimed at evaluating the heat transfer characteristics of water flowing through single and double stack rectangular microchannels of different aspect ratios in electronic cooling applications under different channel height, channel width and bottom wall thickness by uniform heat flux $\dot{q} = 100 \text{ W/cm}^2$ and $Re = 800$. A three-dimensional computational fluid dynamics (CFD) model is built using the commercial package, ANSYS 14.0, to investigate the heat transfer characteristics of water flowing in single and double stack rectangular microchannels heat sink. Results are validated against experimental data obtained by Qu and Mudawar [1] at uniform heat flux, $\dot{q} = 100 \text{ W/cm}^2$ and $Re = 1454$. Nearly uniform temperature profile and low temperature gradient are achieved in counter flow.

KEYWORDS

Heat transfer, Microchannels, Heat sink, Numerical study

* Post Graduate student, Department of Mechanical Power Engineering, Faculty of Engineering at El-Mattaria, Helwan University, Masaken El-Helmia P.O., Cairo 11718, Egypt.

** Assistant Professor, Department of Mechanical Power Engineering, Faculty of Engineering at El-Mattaria, Helwan University, Masaken El-Helmia P.O., Cairo 11718, Egypt.

*** Professor, Department of Mechanical Power Engineering, Faculty of Engineering at El-Mattaria, Helwan University, Masaken El-Helmia P.O., Cairo 11718, Egypt.

NOMENCLATURE

A	Area (m ²)	μ	Dynamic viscosity (kg/m s)
a, b, c	Correlation coefficient	λ	Thermal conductivity (W/m K)
c_p	Specific heat capacity (J/kg k)	ν	kinematic viscosity (m ² /s)
D_h	hydraulic diameter of the fluid flow channel (m)	Subscript	
H	Height or thickness (m)	∞	Ambient
h_{av}	Average heat transfer coefficient (W/m.K)	b	Bottom wall
L	Channel length (m)	ch	Channel
\dot{q}	Heat flux (W/m ²)	i	Direction (x,y,z)
Re	Reynolds number	in	Inlet
U_{in}	Fluid inlet velocity (m/s)	j	Directions (x,y,z)
u, v, w	Velocity in x, y, and z direction	out	Outlet
x, y, z	Cartesian coordinates	s	Solid wall
T	Temperature (K)	th	Thermocouple location
W	Width (m)	t	Top thickness
		u	Unit cell
		0	At inlet x=0

Greek Symbols

α	Aspect Ratio
ρ	density (kg/m ³)

INTRODUCTION

The recent developments in field of microelectronics and ever increasing demand for higher computational speed has intensified power density levels in modern electronic systems. With market trends pushing for tininess, International Technology Roadmap for Semiconductors (ITRS) has predicted that peak power consumption in high performance desktop applications will increase to 198 W by 2015[2] and expected dissipation of heat flux in next generation microprocessors and microelectronic components is over 1000 W/cm² [3]. Consequently, there is an immediate requisite for efficient cooling system to cope with rise in temperature levels by large amount of heat dissipation within a small space. Microchannels, that vary from a fraction of a μm to a few 100s of μm in size, have emerged as a potential solution to these electronic cooling challenges. Non-circular geometries of microchannels are often used because of their relative simplicity in fabrication as compared to circular channels. The substrates used were glass, silicon, stainless steel and copper. Researches indicated that high heat fluxes could be dissipated by a working fluid passing through microchannels that give an increased surface area to volume ratio. In the early 1980s, Tuckerman and Pease [4] reported that a microchannel heat sink could dissipate as much as 790 W/cm² with 71 K mean fluid temperature rise. Due to high heat flux produced by compact integrated circuitries, there is a growing requirement for novel researches into design, performance, and application of microchannel.

Vafai and Zhu [5] proposed a comparison between single and double layer heat sink and indicated that for small temperature variations in the chip, pressure drop required in case of double layer is considerably smaller than single layered structure.

Moreover, it was observed that the stream-wise temperature rise on the base surface substantially reduced compared to that of single layered heat sink. Following this, significant researches have been carried out to further explore the advantages of such kind of system. Recently, Hung et al. [6] numerically analyzed heat transfer characteristics double-layered microchannel heat sink in which the effects of substrate materials, coolants, and geometric parameters such as channel number, channel width ratio, channel aspect ratio, substrate thickness, pumping power, pressure drop, and thermal resistance were investigated. It was found that coolant with high thermal conductivity and low dynamic viscosity and substrate materials having a higher thermal conductivity ratio significantly enhanced the performance of double layer system. The results also revealed enhanced performance of double-layered microchannel heat sink over single layered by an average of 6.3%. It is always necessary to have operating parameters' optimization in any system. According to this, optimization of microchannel (single and double layered system) has also been studied by various authors [7, 8]. As well as investigations of stacked microchannels, in which several layers of heat sinks are located one over another can be found in literature along with their optimization studies [9, 10].

MATERIALS AND METHODS

Description of the Design Cooling Model

The three-dimensional fluid flow and heat transfer in a rectangular copper microchannels heat sink are analyzed using water as the cooling fluid. Figure (1) shows a schematic structure and main dimensions of a rectangular microchannel heat sink. The dimensions' values are listed in Table 1.

Table 1. Dimensions of microchannel heat sink unit cell.

Parameters	Values [mm]
W_{ch}	0.12, 0.15, 0.18, 0.231, 0.225, 0.3
H_{ch}	0.3, 0.4, 0.5, 0.6, 0.7, 0.713
L	44.764
W_u	0.467
W_s	0.118
H	19.05
H_t	12.7
H_b	3.637, 4.637, 5.637, 6.637
H_{th}	3.175

Governing Equation

Table (2) indicates the assumptions used in this study. According to these assumptions the conservation mass, momentum and energy equations, respectively are as follows

$$\frac{\partial}{\partial x_i}(\rho u_i) = 0 \tag{1}$$

$$\frac{\partial}{\partial x_i}(\rho u_i u_j) = -\frac{\partial p}{\partial x_j} + \frac{\partial}{\partial x_i}\left(\mu \frac{\partial u_j}{\partial x_i}\right) + \frac{\partial}{\partial x_i}\left(\frac{\partial u_i}{\partial x_j}\right), j = 1, 2, 3 \tag{2}$$

$$\frac{\partial}{\partial x_i}(\rho u_i T) = \frac{\partial}{\partial x_i}\left[\left(\frac{\lambda}{c_p}\right) \frac{\partial T}{\partial x_i}\right] \tag{3}$$

Table 2. Assumptions

Parameters	Assumptions
Flow characteristics	Three dimensions, steady, incompressible and laminar
Body force	Neglected
Fluid properties	Constant and viscous dissipation is neglected
No slip boundary condition	$u = v = w = 0$, at solid wall [11, 12]
Inlet velocity	Uniform [11, 12]
Microchannels	Identical in heat transfer and flow characteristics (one channel can be investigated) [13]

The boundary conditions for the computational study, indicated in Fig. 1, are provided via experimental data of Qu and Mudawar [1]. The thermo-physical properties of cooling fluid (water) and copper are shown in table (3). These properties are assumed constant due to small variations with the temperature range tested [13]. The governing systems of equations described above are solved using the commercial CFD package, FLUENT 14.0.

Table 3. Thermo-physical Properties of water and copper

Properties	ρ (kg/m ³)	λ (W/mk)	μ (kg/m s)	c_p (J/kg-K)	T (k)
Water	998.2	0.6	0.00103	4182	288
Copper	8978	387.6		381	

RESULTS AND DISCUSSION

An important first step in the computational study as reported in previous related work [11, 13] is to investigate the influence of mesh refinement on the CFD solutions. Accordingly, three different levels of cell volume are used (20, 40 and 60 μm^3). It is found that the maximum percentage change in result is 1.5%. Therefore, the largest size is chosen to save the computing time.

Figure 2 shows that the predictions of temperature along line in x-direction at $H_{th} = 3175 \mu\text{m}$ and the experimental data obtained by Qu and Mudawar [1] at different Reynolds numbers ($Re = 226, 890$ and 1454) and constant uniform heat flux, $\dot{q} = 100 \text{ W/cm}^2$. The results are in reasonably good agreement with experiment. Due to growing boundary layer thickness, the temperature increases along the flow direction and it is extremely high in the outlet region of microchannel.

The channel geometry has a significant effect on the performance of microchannel heat sink. In order to get better thermal performance with mild pressure drop and pumping power, the effects of the thickness from unit cell bottom wall " H_b ", the channel height " H_{ch} " and width " W_{ch} " are deeply investigated at different values listed in table 1. This study is carried out using constant heat flux $\dot{q} = 100 \text{ W/cm}^2$ and Reynolds number of 800. The CFD results present the impact of these parameters on temperature distribution along line in x-direction at $H_{th} = 3175 \mu\text{m}$ and in x-z plane. As well as the effect of geometry parameters on average heat transfer coefficient are addressed.

The hydraulic diameter " D_h " of the fluid flow channel, Reynolds number " Re " and the average heat transfer coefficient " h_{av} " are calculated as follows[14],

$$D_h = \frac{4A}{p} = \frac{4W_{ch}H_{ch}}{2(W_{ch} + H_{ch})} \quad (4)$$

$$Re = \frac{U_m D_h}{\nu} = \frac{U_{in} D_h}{\nu} \quad (5)$$

$$h_{av} = \frac{\dot{q}''}{(T_s - T_\infty)} \quad (6)$$

$$T_\infty = \frac{T_{in} + T_{out}}{2} \quad (7)$$

Effect of Bottom Wall Thickness " H_b "

The effect of bottom wall thickness " H_b " is investigated computationally. Figure 3 shows that the effect of H_b on the temperature distribution (left) at $H_{th} = 3175 \mu\text{m}$ and average heat transfer coefficient " h_{av} " which is calculated and based on the bottom wall of channel (right). It also shows that the influence of H_b is significant and that decreasing the thickness may provide a noticeable cooling enhancement in temperature however, the average heat transfer coefficient decreases. The average heat transfer coefficient variation decreases along the flow direction due to growing boundary layer thickness and extremely high at the entrance region due to the very thin local boundary layer. Figure 4 shows local temperature distributions in x-z plane

for four cases of H_b . The temperature variations are represented by variations in color, with the temperature scale located at the side of each figure. This figure gives detailed information about the temperature distribution in the heat sink.

A general correlation for the variation of the normalized temperature “ T/T_0 ” with H_b/D_h at any location along x-axis is obtained as follows:

$$\frac{T}{T_0} = a + b \left(\frac{x}{L}\right) + c \left(\frac{x}{L}\right)^2 \tag{8}$$

where, T is the temperature at H_{th} along x-axis, T_0 is the inlet fluid temperature at $x=0$ which is used as a reference value (=288 k) and the correlation coefficients a, b and c are given in Table 4.

Table 4. Correlation coefficient A, B and C for normalized temperature Eq. (8).

Correlation coefficients	Restrictions	Adjusted R square
$a = 1.1268 - 0.0029 \left(\frac{H_b}{D_h}\right) - 0.00003 \left(\frac{H_b}{D_h}\right)^2$		
$b = 0.0655 + 0.001 \left(\frac{H_b}{D_h}\right) + 0.00006 \left(\frac{H_b}{D_h}\right)^2$	$q''=100 \text{ W/cm}^2$ $Re= 800$	0.99733
$c = -0.0186 - 0.0004 \left(\frac{H_b}{D_h}\right) - 0.00004 \left(\frac{H_b}{D_h}\right)^2$		

Effect of Channel Height “ H_{ch} ” and Channel Width “ W_{ch} ”

Figures 5 and 6 indicate that the effect of channel height “ H_{ch} ” on the temperature distributions and average heat transfer coefficient at $H_{th}=3175 \mu\text{m}$, $W_{ch}=200 \mu\text{m}$ and $H_b=4637 \mu\text{m}$. Figure 5 depicts that increasing channel height leads to decrease the temperature and increase the average heat transfer coefficient as well as cooling enhancement. In more detail, when H_{ch} increases by 33.33%, 66.67% and 100 %, the average heat transfer coefficient increases by 5.66%, 22.30% and 40.72%, respectively. Figure 7 indicates that the temperature variation contours which show that the best cooling occurs at maximum height of channel.

Similarly, the effect of channel width “ W_{ch} ” on the temperature distributions and average heat transfer coefficient is also investigated at $H_{th}=3175 \mu\text{m}$, $H_{ch}=450 \mu\text{m}$ and $H_b=4637 \mu\text{m}$. As shown in Figs.6 and 8, increasing W_{ch} improves the cooling of heat sink by decreasing the heat sink temperature and increasing of h_{av} . Specifically, increasing width by 20 %, 50% and 100%, the average heat transfer coefficient increases by about 8.20% , 19.39% and 25.50%, respectively.

Similar to Eq. (8), a general correlation for the variation of the normalized temperature “ T/T_0 ” with H_{ch}/D_h and W_{ch}/D_h at any location along x-axis are obtained, respectively as follows:

$$\frac{T}{T_0} = a + b \left(\frac{x}{L}\right) + c \left(\frac{x}{L}\right)^2 \tag{9}$$

where, T is the temperature at H_{th} along x-axis, T₀ is the inlet fluid temperature which is used as a reference value (=288 k) and the correlation coefficients a, b and c for H_{ch}/D_h and W_{ch}/D_h are given in Tables 5 and 6 respectively.

Table 5. Correlation coefficient a, b and c for normalized temperature Eq. (9) for H_{ch}/D_h.

Correlation coefficients	Restrictions	Adjusted R square
$a = 1.2535 - 0.1396 \left(\frac{H_{ch}}{D_h}\right) + 0.0261 \left(\frac{H_{ch}}{D_h}\right)^2$	$q'' = 100 \text{ W/cm}^2$	0.99757
$b = 0.1966 - 0.0667 \left(\frac{H_{ch}}{D_h}\right) + 0.0081 \left(\frac{H_{ch}}{D_h}\right)^2$	Re = 800 W _{ch} = 200 μm	
$c = -0.062 + 0.0162 \left(\frac{H_{ch}}{D_h}\right) - 0.0012 \left(\frac{H_{ch}}{D_h}\right)^2$	H _b = 4637 μm	

Table 6. Correlation coefficient a, b and c for normalized temperature Eq. (9) for W_{ch}/D_h

Correlation coefficients	Restrictions	Adjusted R square
$a = 0.954 + 0.3233 \left(\frac{W_{ch}}{D_h}\right) - 0.1785 \left(\frac{W_{ch}}{D_h}\right)^2$	$q'' = 100 \text{ W/cm}^2$	0.99856
$b = -0.8018 + 2.2372 \left(\frac{W_{ch}}{D_h}\right) - 1.3423 \left(\frac{W_{ch}}{D_h}\right)^2$	Re = 800 H _{ch} = 450 μm	
$c = 0.4785 - 1.2603 \left(\frac{W_{ch}}{D_h}\right) + 0.7483 \left(\frac{W_{ch}}{D_h}\right)^2$	H _b = 4637 μm	

Effect of Double Stack Rectangular Microchannel and Flow Direction

Figures 9 show the temperature contours for double stack in x-z plane at H_{th}=3175 μm, H_{ch}=700 μm, W_{ch}=200 μm, H_b=4637 μm, q̇ = 100 W/cm² and Re = 800 for parallel and counter flow. As shown in the Figures, the parallel flow the temperature of the heat sink near to the coolant inlet is less than the temperature at coolant outlet. This significant change in heat sink temperature profile is due to the coolant temperature increase at microchannels outlet. On the other hand, in the counter flow the temperature profile in heat sink has a symmetrical profile. Figure 10 indicates that double stack microchannel is better than single microchannel by about 7% cooling enhancement. In addition, the temperature gradients in the counter flow are less

than the parallel flow. As a result, counter flow is more suitable for microchannel cooling process.

CONCLUSION

The combined conduction–convection heat transfer in the microchannel produces a very complex three dimensional heat flow pattern with large, longitudinal, upstream directed heat recirculation zones in the highly conducting copper substrate, in which the fluid and solid are in direct contact. A computational fluid dynamics approach, based on Fluent is capable of predicting the temperature distribution and average heat transfer coefficient. Complementary CFD results show that the forced convection water cooled microchannel heat sink has a superior potential for application in thermal management of the electronic packages. The microchannels geometry has a significant influence on the cooling process. Decreasing the bottom wall thickness improves the cooling process through a reduction in the temperature of heat sink.

In addition, increasing both channel height and channel width enhances cooling process due to increasing the heat transfer coefficient. The average heat transfer coefficient is improved by 5.66%, 22.3% and 40.72% when the channel height is increased by 33.33%, 66.67% and 100%. While if the channel width is increased by 20%, 50% and 100%, the heat transfer coefficient increases by 8.2%, 19.39% and 25.5%.

Moreover, in double stack microchannels the counter water flow direction is more suitable in cooling process than the parallel flow due to uniform temperature distribution and low temperature gradient.

REFERENCES

- [1] W. Qu and I. Mudawar, "Experimental and numerical study of pressure drop and heat transfer in a single-phase micro-channel heat sink", *International Journal of Heat and Mass Transfer* 45, 2002, pp 2549-2565
- [2] "2007 International Technology Roadmap for Semiconductors, Executive Summary," 2007.
- [3] L. Chai, G. Xia, M. Zhou, and J. Li, "Numerical simulation of fluid flow and heat transfer in a microchannel heat sink with offset fan-shaped reentrant cavities in sidewall", *International Communications in Heat and Mass Transfer*, vol. 38, 2011, pp 577-584.
- [4] B. D. Tuckerman and R. F. W. Pease, "High-performance heat sinking for VLSI", *IEEE Electr. Device Lett. EDL*, vol. 2, 1981, pp 136-147.
- [5] K. Vafai and L. Zhu, "Analysis of two-layered microchannel heat sink concept in electronic cooling", *International Journal of Heat and Mass Transfer*, vol. 42, 1999, pp 2287-2297.
- [6] T. C. Hung, W. M. Yan and W. P. Li, "Analysis of heat transfer characteristics of double-layered microchannel heat sink," *International Journal of Heat and Mass Transfer*, vol. 55, 2012, pp 3090-3099.

- [7] S. H. Chong, K. T. Ooi, and T. N. Wong, "Optimisation of single and double layer counter flow microchannel heat sinks", *Applied Thermal Engineering*, vol. 22, 2002, pp 1569-1585.
- [8] K. Jeevan, I. A. Azid and K. N. Seetharamu, "Optimization of double layer counter flow (DLCF) micro-channel heat sink used for cooling chips directly", in *Electronics Packaging Technology Conference*, 2004, pp 553-558.
- [9] X. Wei and Y. Joshi, "Optimization study of stacked microchannel heat sinks for micro-electronic cooling", in *Thermal and Thermomechanical Phenomena in Electronic Systems, The Eighth Intersociety Conference on*, 2002, pp 441-448.
- [10] X. Wei and Y. Joshi, "Stacked Microchannel Heat Sinks for Liquid Cooling of Microelectronic Components", *Journal of Electronic Packaging*, vol. 126, 2004, pp 60-66.
- [11] S.V. Patankar, "Numerical Heat Transfer and Fluid Flow", Hemisphere, NY, 1980.
- [12] W.Q. Tao, "Numerical Heat Transfer", second ed., Xi'an Jiaotong University Press, Xi'an, China, 2001.
- [13] X. L. Xie, Z. J. Liu, Y. L. He and W. Q. Tao, "Numerical study of laminar heat transfer and pressure drop characteristics in a water-cooled minichannel heat sink", *Applied thermal engineering*, vol. 29, 2009, pp 64-74.
- [14] O. Levenspiel, "Engineering Flow and Heat Exchange", 2nd Edition, Plenum Press, 1998

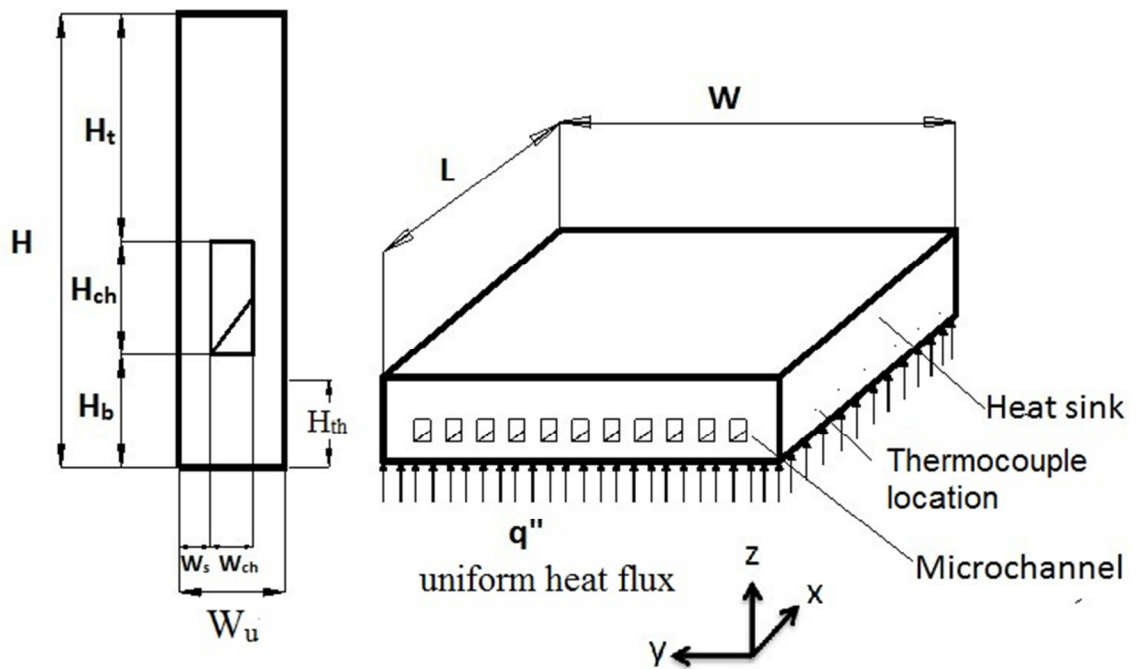


Fig. 1. Schematic of the microchannel heat sink.

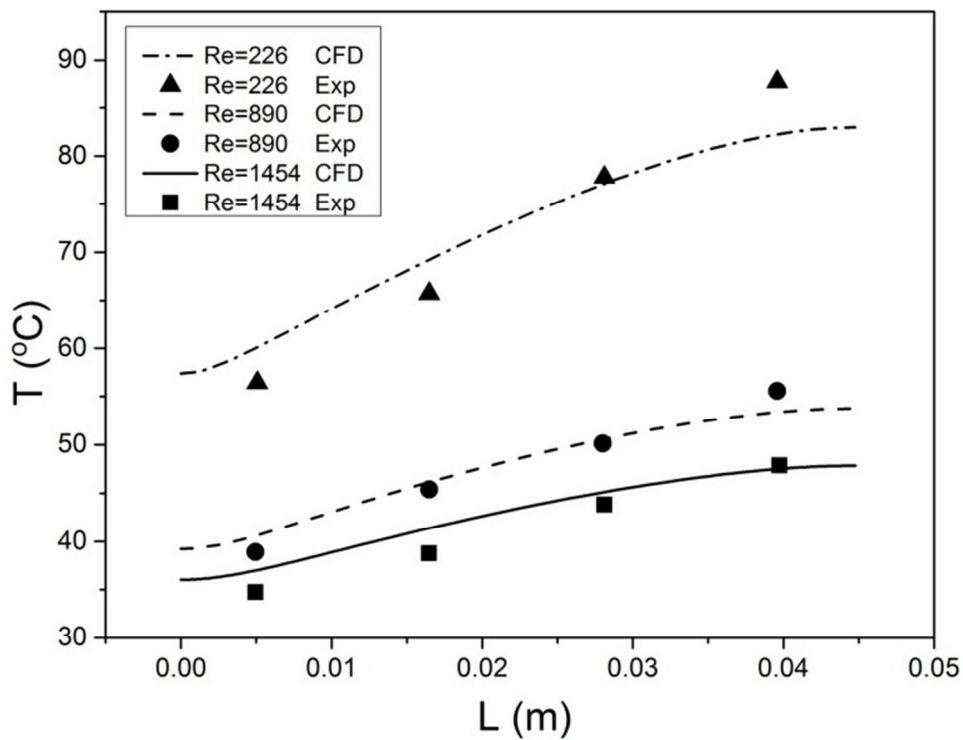


Fig. 2. Comparison of experimental data [1] and predictions for temperature distribution along line in x-direction at $H_{th} = 3175 \mu\text{m}$, heat flux $\dot{q} = 100 \text{ W/cm}^2$ and $Re = 226, 890$ and 1454

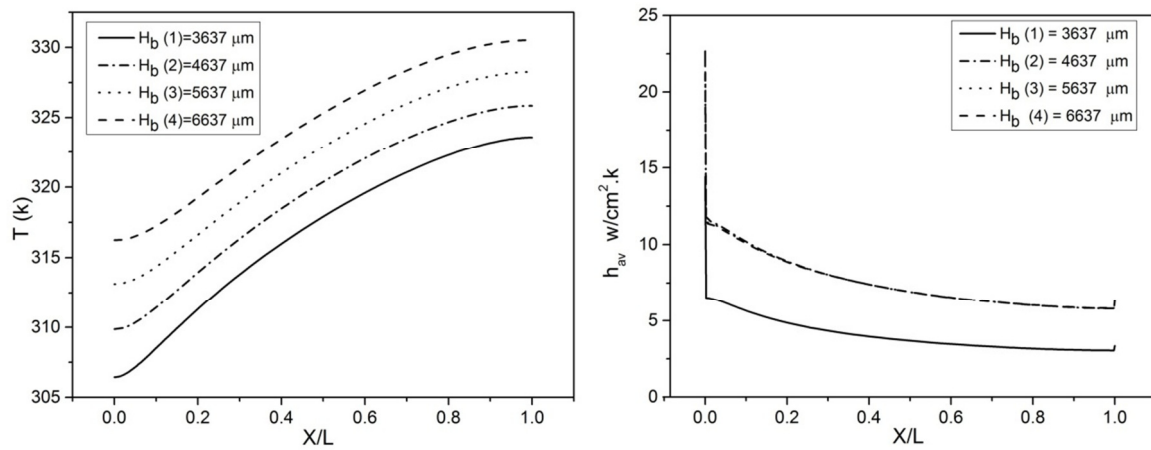


Fig. 3. Effect of bottom thickness “ H_b ” on temperature distribution and heat transfer coefficient at $H_{th}=3175 \mu\text{m}$, $\dot{q} = 100 \text{ W}/\text{cm}^2$ and $\text{Re} = 800$.

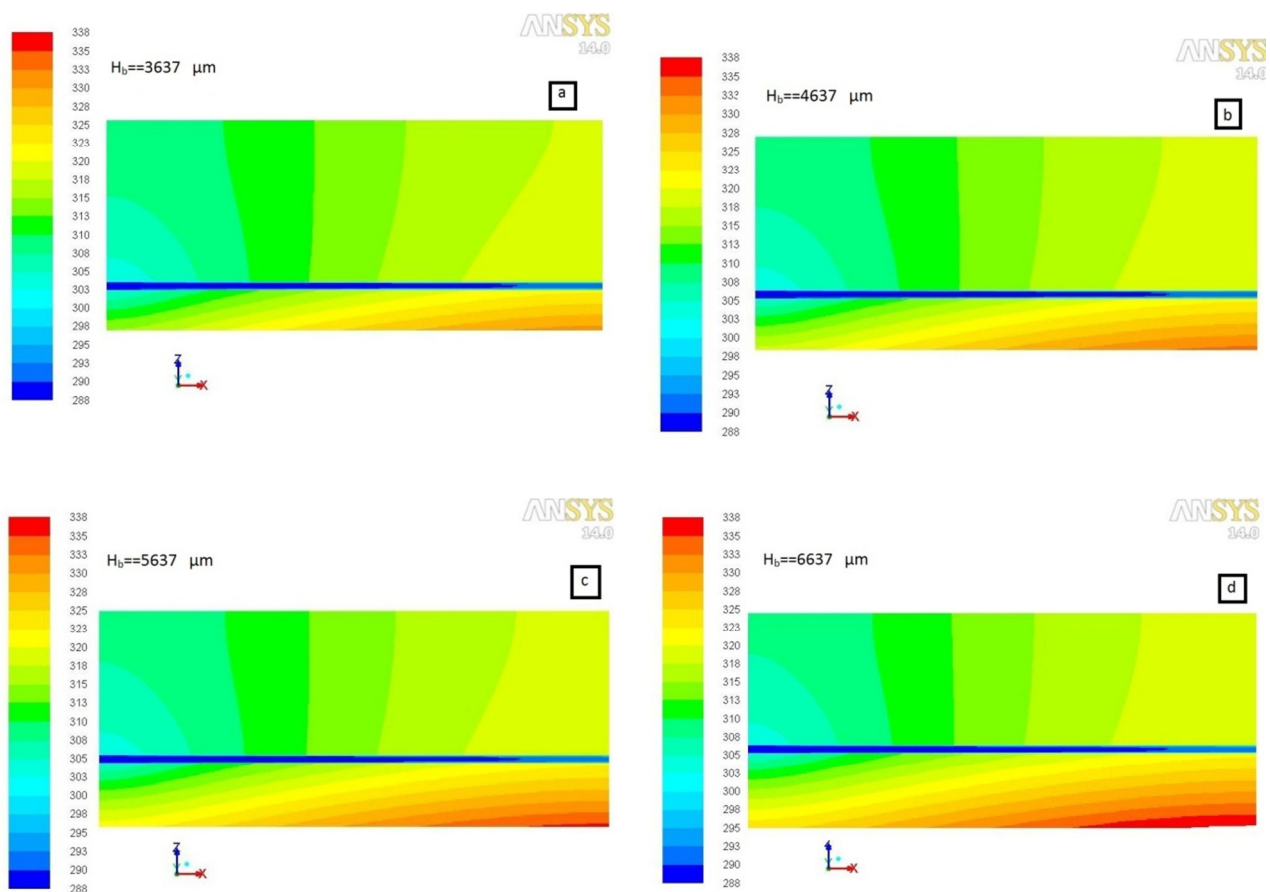


Fig. 4. Local temperature distribution in x - z plane at $y=W_u/2$, different bottom thickness, $\dot{q}=100 \text{ W}/\text{cm}^2$ and $\text{Re} = 800$.

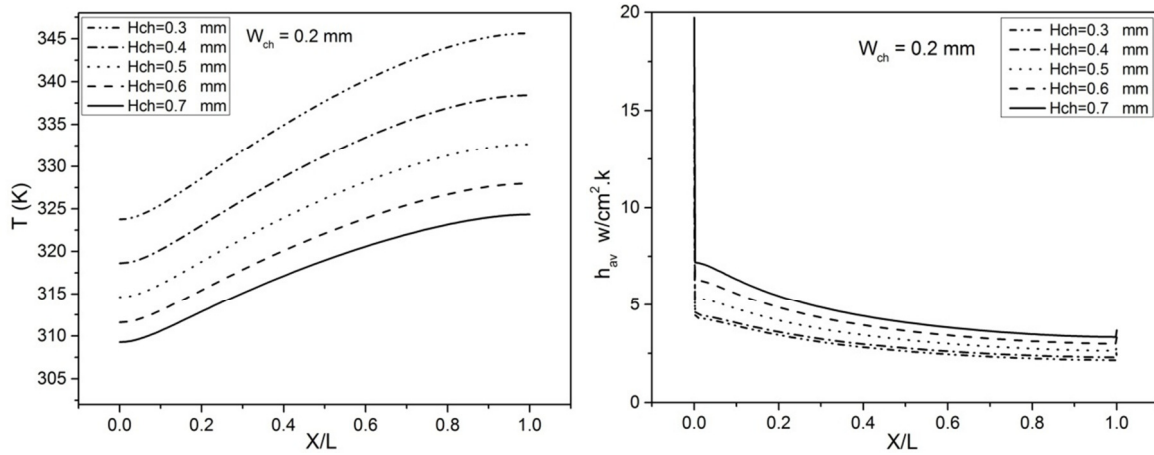


Fig. 5. Effect of channel height “ H_{ch} ” on temperature distribution and heat transfer coefficient at $H_{th}=3175 \mu\text{m}$, $W_{ch}=200 \mu\text{m}$, $H_b=4637 \mu\text{m}$, $\dot{q} = 100 \text{ W/cm}^2$ and $Re = 800$.

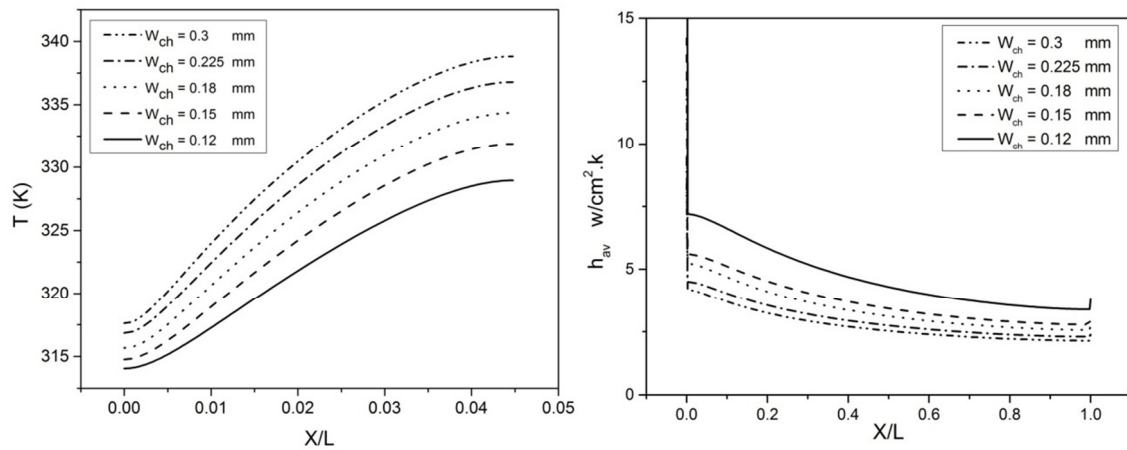


Fig. 6. Effect of channel width “ W_{ch} ” on temperature distribution and heat transfer coefficient at $H_{th}=3175 \mu\text{m}$, $H_{ch}=450 \mu\text{m}$, $H_b=4637 \mu\text{m}$, $\dot{q} = 100 \text{ W/cm}^2$ and $Re = 800$.

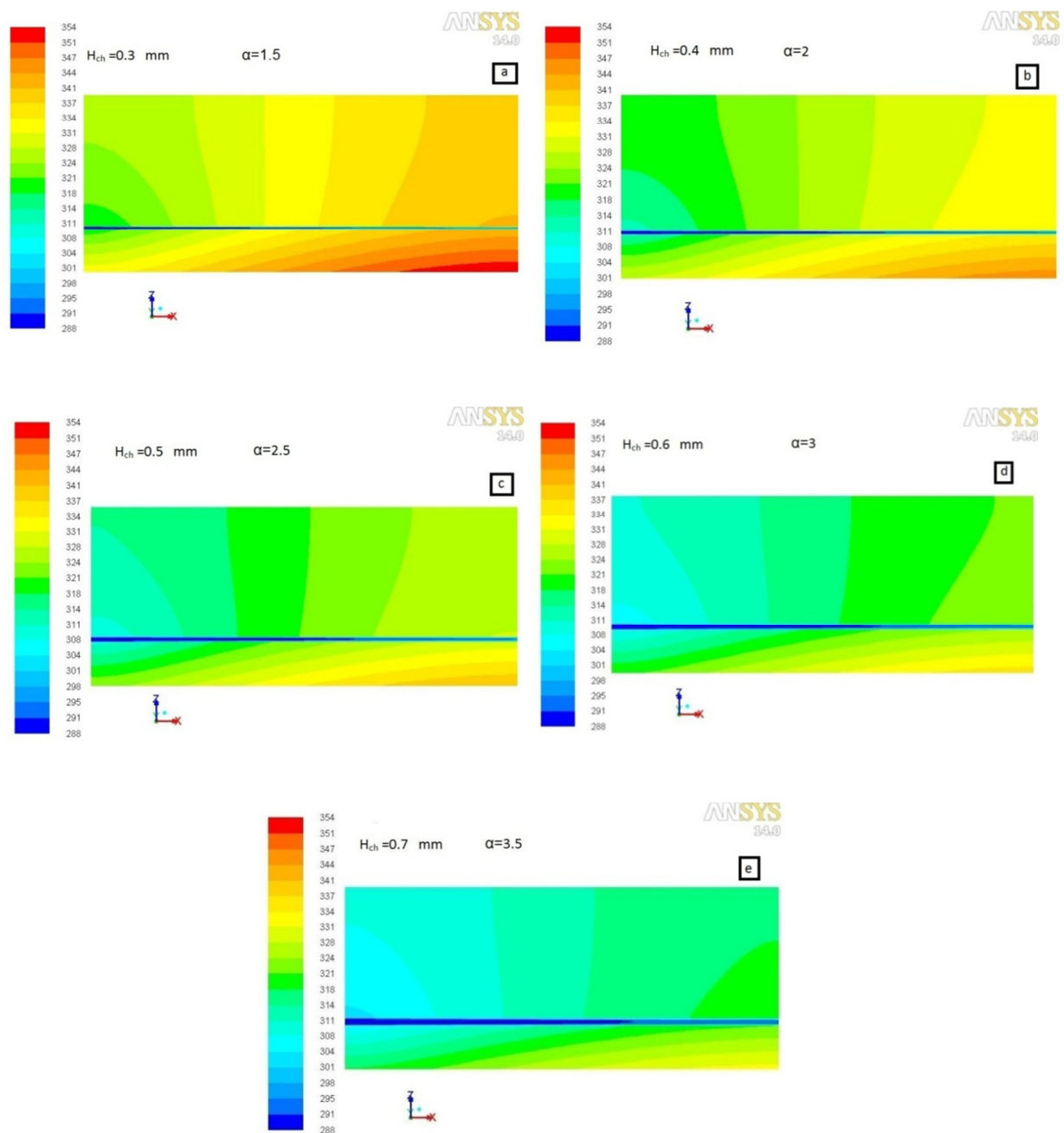


Fig. 7. Local temperature distribution in x-z plane at $y=W_u/2$, different channel height, $H_{th}=3175 \mu\text{m}$, $W_{ch}=200 \mu\text{m}$, $H_b=4637 \mu\text{m}$, $\dot{q} = 100 \text{ W/cm}^2$ and $Re = 800$
 $\dot{q}=100 \text{ W/cm}^2$ and $Re=800$.

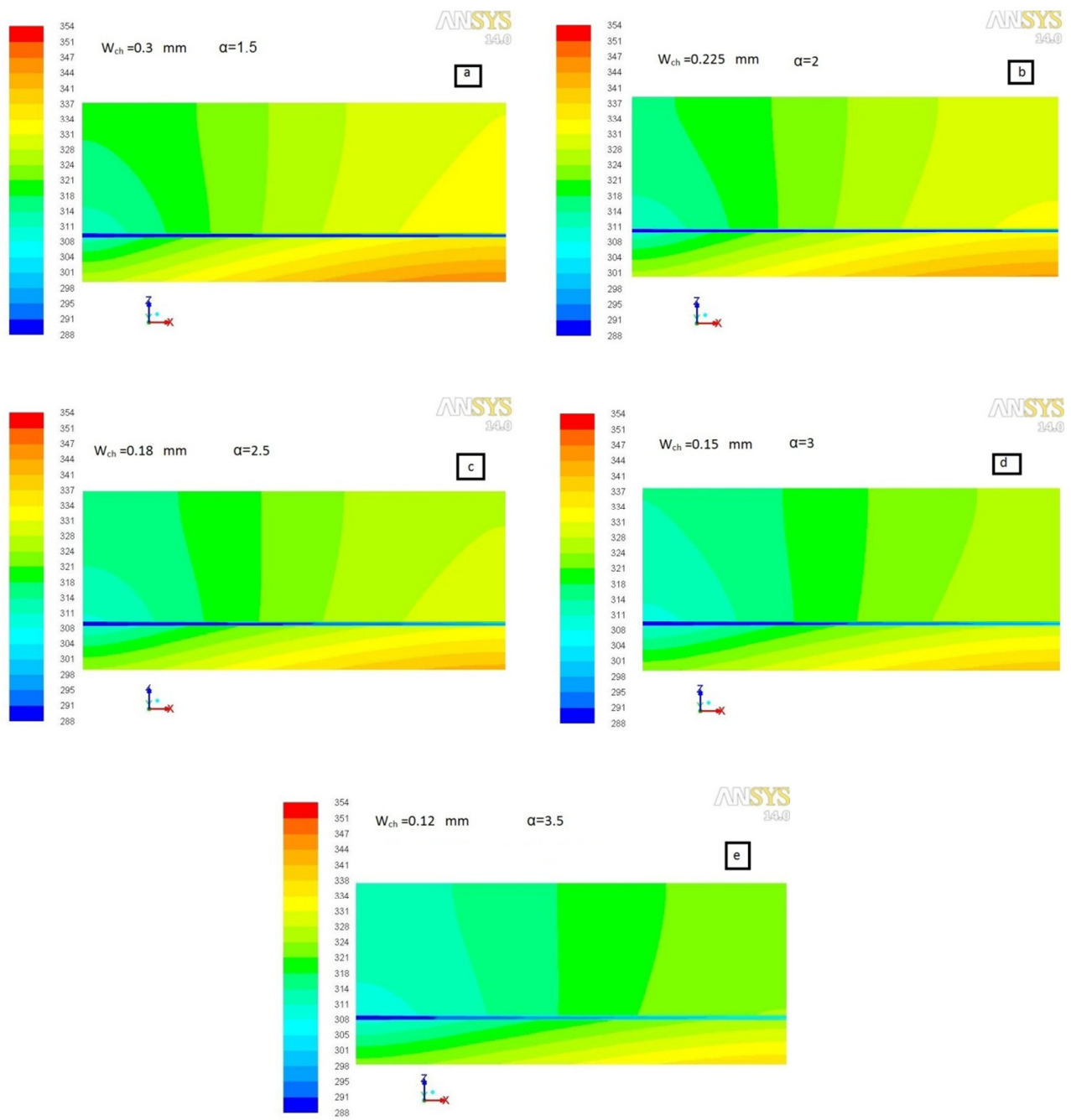


Fig. 8. Local temperature distribution in x-z plane at $y=W_u/2$, different channel height, $H_{th}=3175 \mu\text{m}$, $H_{ch}=450 \mu\text{m}$, $H_b=4637 \mu\text{m}$, $\dot{q} = 100 \text{ W/cm}^2$ and $Re = 800$.

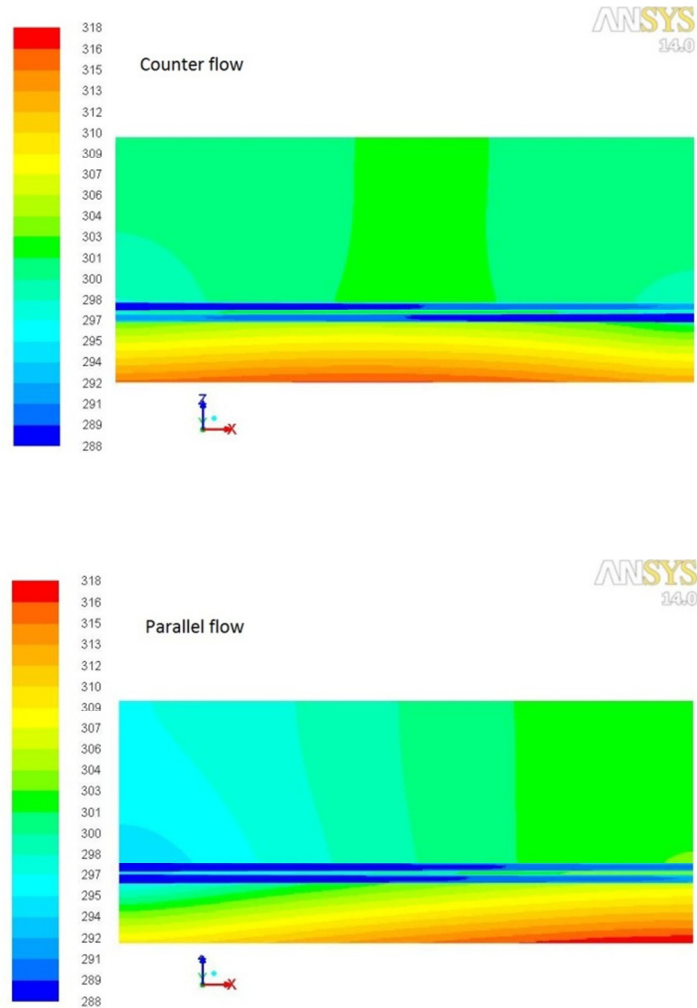


Fig. 9. Local temperature distribution in x-z plane at $y=W_u/2$, $H_{th}=3175 \mu\text{m}$, $H_{ch}=700 \mu\text{m}$, $H_b=4637 \mu\text{m}$, $W_{ch}=200 \mu\text{m}$, $\dot{q} = 100 \text{ W/cm}^2$ and $Re = 800$ for counter and parallel flow

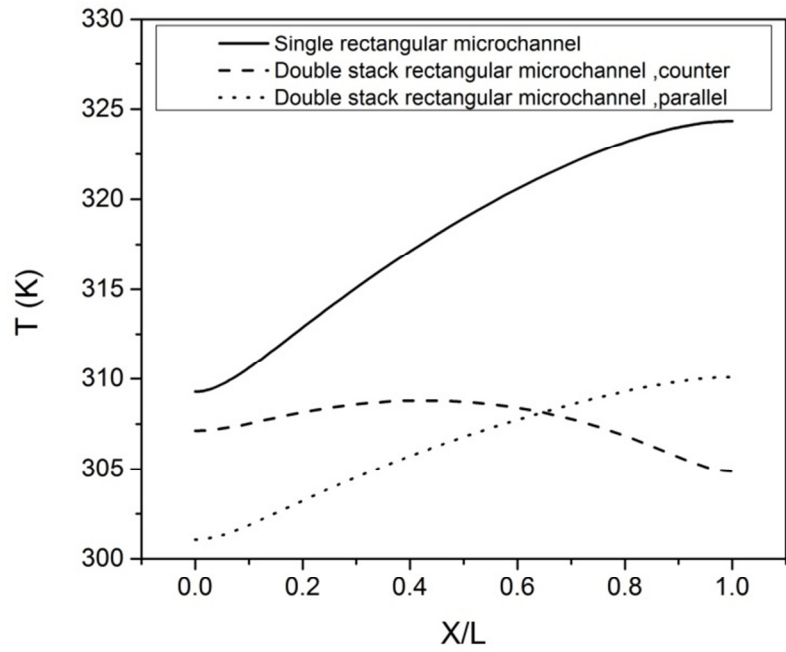
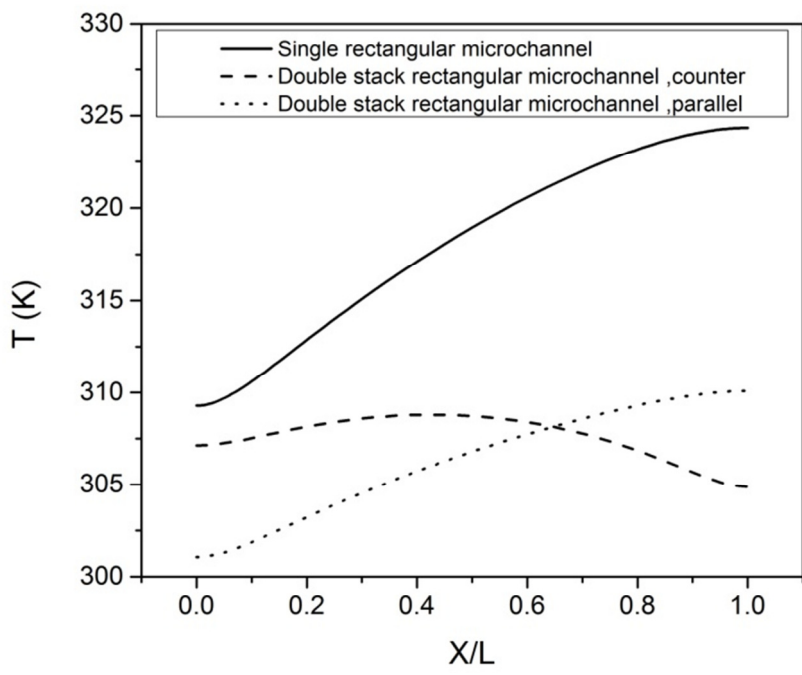


Fig. 10. Effect of water flow direction in double stack rectangular microchannels on temperature distribution at $H_{th}=3175 \mu\text{m}$, $H_{ch}=700 \mu\text{m}$, $W_{ch}=200 \mu\text{m}$, $H_b=4637 \mu\text{m}$, $\dot{q} = 100 \text{ W/cm}^2$ and $Re=800$